Human mesenchymal stromal cell adhesion and expansion on fluoropolymer surfaces modified with oxygen and nitrogen-rich plasma polymers

Balaji Ramachandran [a†], *Gad Sabbatier* [a†], *Olivia M. Bowden* [a], *Katie Campbell* [b], *Natalie Fekete* [b], *Pierre-Luc Girard-Lauriault* [a], *Corinne A. Hoesli* [a*]

[a]Department of Chemical Engineering, McGill University, Montréal, Canada

[b]Saint-Gobain Ceramics & Plastics, Inc., Northboro R&D Center, Northborough, Massachusetts

[*]Correspondence: Corinne Hoesli, Department of Chemical Engineering, McGill University, Montréal, QC, Canada H3A 0C5. Email id: corinne.hoesli@mcgill.ca Tel no: 5143984275

[†]These authors contributed equally to this work.

This article has been accepted and published in the Journal "Colloids and Surfaces B: Biointerfaces" DOI: https://doi.org/10.1016/j.colsurfb.2023.113740

Abstract:

Fluorinated ethylene propylene (FEP) vessels are of significant interest for therapeutic cell biomanufacturing applications due to their chemical inertness, hydrophobic surface, and high oxygen permeability properties. However, these properties also limit the adhesion and survival of anchorage-dependent cells. Here, we develop novel plasma polymer coatings to modify FEP surfaces, enhancing the adhesion and expansion of human mesenchymal stromal cells. Similar to commercially available tissue culture polystyrene vessels, oxygen-rich or nitrogen-rich surface chemistries can be achieved using this approach. While steam sterilization increased the roughness of the coatings and altered the surface chemistry, the overall wettability and oxygen or nitrogen-rich nature of the coatings were maintained. In the absence of proteins during initial cell attachment, cells adhered to surfaces even in the presence of chelators, whereas adhesion was abrogated with chelator in a protein-containing medium, suggesting that integrin-mediated adhesion predominates over physicochemical tethering in normal protein-containing cell seeding conditions. Albumin adsorption was more elevated on nitrogen-rich coatings compared to the oxygen-rich coatings, which was correlated with a higher extent of hMSC expansion after 3 days. Both the oxygen and nitrogen-rich coatings significantly improved hMSC adhesion and expansion compared to untreated FEP. FEP surfaces with nitrogen-rich coatings were practically equivalent to commercially available standard tissue culture-treated polystyrene surfaces in terms of hMSC yields. Plasma polymer coatings show significant promise in expanding the potential usage of FEP-based culture vessels for cell therapy applications.

Keywords: Surface modification, Fluorinated ethylene propylene, Plasma polymer coatings, Steam sterilization, human mesenchymal stromal cells

Graphical abstract:

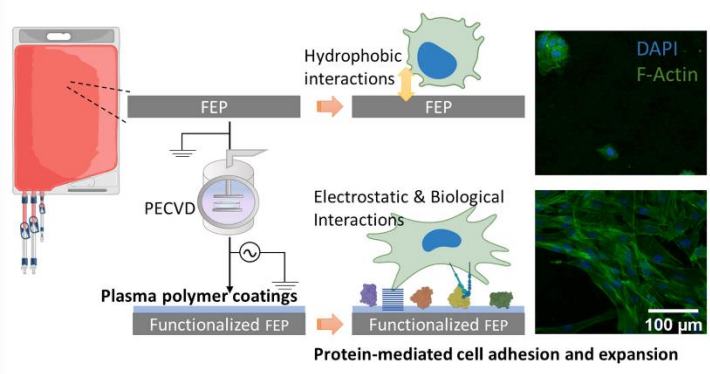

Abbreviations: PECVD, Plasma-enhanced Chemical Vapour Deposition; PPCs, Plasma Polymer Coatings; FEP, Fluorinated Ethylene Propylene; hMSC, human mesenchymal stromal cell.

1. Introduction:

Cell-based therapies have shown promise in addressing complex degenerative diseases through their dynamic ability to respond to chemical, physical, and biological cues and multifaceted functional attributes [1]. Compared to more conventional biomanufacturing approaches, challenges related to in-process variability, storage and handling are exacerbated with living cell products. The biomanufacturing process involves a series of upstream and downstream unit operation processes from the isolation of donor cells, cell expansion, medium exchange, harvest, formulation, storage, distribution and administration of the cell-based products to the patient [2]. Implementing current good manufacturing practices (cGMP) is essential to ensure consistent quality and safety of therapeutic cell products. Closed culture systems aid in implementing cGMP by reducing the risk of contamination, improving product consistency, and reducing failure of production runs in clinical settings [3]. The fluoropolymers used in various biomedical applications have promising potential as closed culture systems. Among the fluoropolymers, fluorinated ethylene propylene (FEP) bags are gaining popularity as closed culture single-use vessels because of their high oxygen permeability, chemical stability, absence of leachables, thermal resistance, and light transmission [4]. In cell culture applications, some advantages of using FEP bags over traditional polystyrene flasks are uniform gas exchange, high flexural strength, reduced evaporation, and a closed system that improves overall functionality [5]. FEP bags have mainly been implemented in the culture of anchorage-independent cells such as monocytes [6], dendritic cells [7, 8], CAR-T cells [9, 10] and myeloma [11, 12]. The inert and hydrophobic nature of FEP is inadequate for the adhesion and growth of anchorage-dependent cells such as human mesenchymal stromal cells (hMSCs).

The multipotent nature and immunomodulatory features of hMSCs are being explored for the treatment of neurodegenerative, autoimmune, cardiovascular, liver, bone, and cartilage diseases

[13, 14]. From the first clinical trial reported in 1995, the number of registered trials of hMSC has significantly increased to 1,542 (*clinicaltrials.gov)* in 2023 [15]. This year, the field is anticipating the approval of Mesoblast's Remestemcel-L. If approved, it will be the first allogeneic "Off-the-Shelf" cellular medicine in the United States, and the first therapy for children under 12 years old with steroid-refractory acute graft versus host disease [16]. Despite their wide range of potential applications, the availability of hMSCs is limited, ranging from 0.0017% – 0.0201% of the total bone marrow mononuclear cells [17]. Expanding isolated hMSC is crucial for therapeutic applications at clinical scale. FEP culture vessels for adherent cell culture are commercially available from Saint-Gobain Life Sciences as VueLife® "AC" series bags [18]. In an effort to further expand our understanding of culturing anchorage-dependent cells in these systems, this research article focuses on novel plasma-modified FEP surfaces and studying their properties that affect cell-material interactions.

Plasma treatment is one of the most effective methods for surface modification of materials. Specifically, plasma polymerization techniques are increasingly [19] being applied to engineer material surfaces for introducing different functional groups, thereby influencing cell-surface interactions and culture outcomes [20]. The surfaces of polymeric biomaterials have been altered using different plasma treatments to improve cell adhesion and hemocompatibility, or to hinder fouling and bacterial adhesion [21, 22]. Plasma polymerization is a promising approach for FEP surface modification if challenges related to retaining surface functionality and coating stability under cGMP-compliant sterilization methods can be addressed [23, 24]. A better understanding of the effect of plasma coated FEP surface properties on protein adsorption, cell adhesion mechanisms and cell growth behavior would provide confidence in the development of these materials for clinical-grade production of hMSCs and other anchorage-dependent cells.

In this work, we used plasma-enhanced chemical vapor deposition (PECVD) to modify FEP surfaces. Oxygen-rich plasma polymer coatings (O-rich PPCs) and nitrogen-rich plasma polymer coatings (N-rich PPCs) were deposited using three gas mixtures (ethylene/ammonia/carbon dioxide). After plasma treatment, the surface properties were investigated pre- and post-sterilization. X-ray photoelectron spectroscopy (XPS), water contact angle, and atomic force microscopy (AFM) were used to characterize the modified surface properties. Albumin adsorption on O-rich and N-rich PPCs was studied through quartz crystal microbalance with dissipation monitoring. The adhesion and expansion of hMSCs were quantified on O-rich and N-rich PPCs in comparison with commercially available tissue culture-treated polystyrene (TCPS) surfaces. When probing hMSC adhesion mechanisms in protein-free vs protein-containing conditions, a surprising finding was that hMSCs tethered efficiently to FEP in the absence of proteins even in the presence of a chelator, contrary to observations in protein-containing medium. FEP surfaces with N-rich coatings showed higher levels of albumin adsorption than for O-rich coatings, which was correlated with higher 3-day hMSC expansion, reaching levels that were practically equivalent to those observed on TCPS.

2. Experimental details:

2.1. Surface modification by plasma treatment

FEP films of 0.005” thickness were provided by Saint-Gobain Life Sciences, Northborough, MA, USA. The unmodified FEP surfaces were cleaned in 70% ethanol followed by reverse osmosis (RO) water and then vacuum dried overnight. The surface of the FEP was modified using an in-house PECVD reactor [25] that was extensively characterized. The surfaces were initially plasma pretreated with ammonia gas (15 sccm flow rate and 13.3 Pa pressure) at 60 W power for

45 s to improve the cohesion between substrate FEP and plasma polymer layer. Immediately after the pretreatment, O-rich and N-rich PPCs were deposited using three gas mixtures (ethylene, C_2H_4 / ammonia, NH_3 / carbon dioxide, CO_2) described in Table 1. After the plasma treatment, modified samples were sealed in low oxygen transmission rate bags inside an inert glovebox with an argon atmosphere, followed by storage at -40 °C until further use [26].

Table 1. Plasma conditions for the deposition of PPCs on the FEP surface

Plasma treatment	RF power (W)	Pressure (Pa)	Time (min)	Flow rates (sccm)		
				C_2H_4	NH_3	CO_2
O-rich PPCs	20	80	15	20	5	20
N-rich PPCs	20	80	15	20	10	2

2.2. Surface characterization of modified FEP surfaces

The surface elemental composition of unmodified and plasma polymer-coated FEP surfaces was identified using an XPS instrument (Thermo Scientific K-Alpha™) equipped with monochromatic A1 Kα radiation. The surface composition was determined using Thermo Fisher Scientific Avantage Software (version: 5.9922).

Chemical derivatization coupled XPS analysis was used to determine the percentage of the carboxylic (-COOH) and amines ($-NH_2$) functional groups on the PPC surface. To estimate -COOH groups, the samples were immersed in aqueous silver nitrate ($AgNO_3$) solution (1.2 M) for 90 min at pH 6, allowing the formation of carboxylate ions (COO^-Ag^+) with silver as a counterion. Samples were then washed thoroughly with water and dried at 40 °C overnight in a desiccator before being taken for XPS analysis. The percentage of silver (Ag) detected in XPS was then correlated to the amount of surface carboxylic acid groups [27]. To estimate $-NH_2$ groups, the samples were incubated with 4-(trifluoromethyl) benzaldehyde (TFBA) in the vapour phase for 3

h at 45 °C. Though fluorine tagged aldehydes can bind to amines and imines [28], other nucleophilic groups with reactivity towards aldehydes will contribute to the signal. The percentage of -NH_2 (and other aldehyde-reactive nucleophiles) can be calculated using the following equation [25],

$$[NH_2]_u = [N]_u \times \frac{[F]_d}{3[N]_d}$$

Where subscripts u and d refer to underivatized and derivatized samples, respectively.

The stability of these coatings in air and inert storage environment conditions was investigated. After deposition (Day 0), the PPCs were sterilized and stored in two different conditions: air and inert argon environment at room temperature. XPS and water contact angle measurements were performed on these conditions on days 1, 3, 5, and 7 to understand the short- and long-term aging effects. Wettability was measured using a contact angle goniometer (Future Digital Scientific Corp.) connected to a video camera system and computer software (SCA 2.0). A 5 µL water droplet was deposited on the surface using an automated sessile drop method.

The surface topography was determined using MFP-3D SA atomic force microscopy. The AFM images were taken in AC mode (tapping) using a silicon ACTA cantilever (300 kHz, R<10 nm, AppNano). The root mean square roughness of the unmodified and modified FEP surfaces was calculated using Igor Pro software (WaveMetrics).

2.3. Sterilization of plasma polymer coated surfaces

To study the effect of sterilization on PPCs, the modified samples were autoclaved using standard sterilization of 15 min at 121 °C and 15 PSI [29]. After steam sterilization, the surface properties of the samples were characterized by XPS, water contact angle analysis, and AFM. To

understand the hydrophobic recovery due to aging, the samples were immersed in RO water for 1 h and dried before measuring water contact angles.

2.4. Quartz Crystal Microbalance with Dissipation Monitoring (QCM-D)

Human serum albumin adsorption kinetics on O-rich and N-rich PPC surfaces was studied using QCM-D assays on plasma polymer-coated gold crystals. The uncoated gold surface QCM-D crystals (QSX 301, Biolin Scientific) was placed in the PECVD reactor and coated using conditions as Table 1 with different flow rate of PP 20:10:10 ($C_2H_4/NH_3/CO_2 \rightarrow 20/10/10$ sccm). QCM-D experiments were performed with a Q-Sense E1 QCM-D (Biolin Scientific) equipped with a Q-Sense flow module and a peristaltic pump. The QCM-D temperature was equilibrated at 22 °C, and the solutions were filtered with a 0.1 µm Millipore filter. O-rich and N-rich surfaces were developed by submerging the crystals in phosphate-buffered saline (PBS) for 3 h and 24 h in static conditions. Then the crystal was exposed to a 10 ng/mL human serum albumin solution (#A9080, Sigma Aldrich) for about 3 h at a flow rate of 0.1 mL/min. The change in frequency of the crystals was recorded and analyzed.

2.5. Human Mesenchymal Stromal Cell Adhesion Assay

Primary hMSCs from different donors (3 female and 2 male of age between 19 to 35 Y) at passage 2 were obtained from Lonza (PT-2501). Cryopreserved bone marrow-derived hMSCs from passages 3 and 4 were thawed and cultured in serum- and xeno-free MSC expansion medium (#130-104-182, StemMACS™ Miltenyi Biotec). Untreated FEP, as well as FEP films with O-rich PPCs and N-rich PPCs were sterilized and mounted on the removable chamber slides (CultureWell™ Grace Bio-Labs), while TCPS (Nunclon Delta Surface) was used as control. Nunclon® Delta is a cell culture–treated surface modification, which makes the TCPS more

hydrophilic for promoting maximum adhesion and spreading [30]. The cells were grown on the T-75 flasks to reach 80% confluence and then detached from the surfaces using TrypLE™ Express (#12605028, Gibco™). TrypLE action was inhibited using StemMACS™ media before centrifuging the cells at 300 x g for 5 min. The cells were washed once in StemMACS™ media and then seeded on the sample surfaces at 5,000 cells/cm^2 in 500 µL/cm^2 culture surface. The seeded cells were incubated in a humidified atmosphere containing 5% CO_2 at 37 °C. On days 1 and 3, the non-adhered cells were removed from the surface by rinsing twice with Dulbecco's phosphate-buffered saline solution (DPBS). Subsequently, the adherent cells were fixed with 4% paraformaldehyde (#J61899, ThermoFisher Scientific) in PBS for 15 min at room temperature, washed and stored in DPBS solution until staining.

Fixed samples were permeabilized with 0.1% Triton-X (#T8787, Sigma-Aldrich®) in DPBS for 15 min, and surfaces were then washed with 0.05% Tween-20 (#P9416, Sigma-Aldrich®) wash buffer. Then the samples were incubated in Dako protein block (Agilent Technologies, Inc) for 15 min at room temperature. The actin cytoskeleton was stained with 50 µg/mL fluorescein isothiocyanate labelled phalloidin (#P5282 Sigma Aldrich). Samples were incubated for 2 h at room temperature in the dark. Subsequently, adhered cell nuclei were stained with 1 µg/mL of 4′,6-diamidino-2-phenylindole (DAPI, #D9542, Sigma-Aldrich®) for 15 min at room temperature in the dark. Samples were washed with RO water and stored in DPBS at 4° C in the dark until imaging. Twenty-one images per well were taken via an Olympus IX81 fluorescence microscope equipped with a programmable Prior® stage (Prior Scientific Inc., Rockland, MA). The adherent cell density was calculated by counting the DAPI-stained nuclei in the captured images using "analyze particle" tools on Fiji ImageJ.

2.6. Characterization of hMSCs through flow cytometric analysis of surface markers

The hMSCs were trypsinized on day 3, centrifuged at 500 ×g for 5 min and resuspended in FACS buffer (DPBS supplemented with 0.5% bovine serum albumin and 2 mM ethylenediaminetetraacetic acid (EDTA) sodium salt). Then, a volume of 2 µL per million cells of a human Fc block solution (BD Biosciences) was added and the solution was incubated for 10 min at room temperature. A panel of surface markers was used to characterize bone marrow-derived hMSCs as recommended by the International Society for Cell & Gene Therapy [31], including CD105 (561443, BD Biosciences), CD73 (344004, Biolegend), CD90 (328108, Biolegend), CD19 (392506, Biolegend), CD34 (555821, Biolegend), CD14 (367116, Biolegend), CD45 (560975, Biolegend) and HLA-DR (555812, Biolegend). A volume of 0.8 µL of fixable viability stain 660 (BD Biosciences) was added to each sample to discriminate dead cells. Samples were incubated at 4 °C for 20 min. Cells were then centrifuged at 300 ×g for 2 min and resuspended in fresh FACS buffer before flow cytometry on a BD Accuri instrument. Compensation controls were also included (ultraComp eBead, Invitrogen) to correct spectral overlap between the fluorescein (FITC) and the phycoerythrin (PE). The flow cytometry data were analyzed with Flow Jo (LLC).

2.7. Chelation assay to study cell adhesion mechanisms

The basal StemMACS™ medium was used as protein-free media, and the basal media with protein supplement was used as protein-containing media for this assay. Before the inhibition study, EDTA (#15575020, Invitrogen™) of different concentrations (0, 1, 5, 10 mM) was added to the protein-free and protein-containing StemMACS™ medium and incubated overnight at 37 °C and 5% CO_2. On the day of the experiment, hMSCs were incubated in the pre-equilibrated media at room temperature for 10 min before seeding. The cells were seeded on FEP (untreated),

FEP with O-rich PPCs, FEP with N-rich PPCs and TCPS (Nunclon Delta) surfaces at a density of 15,000 cells/cm^2. The seeded cells were incubated in a humidified atmosphere containing 5% CO_2 at 37 °C. After 2 h, the non-adhered cells were removed from the surface by rinsing twice with DPBS. Subsequently, the adherent cells were fixed with 4% paraformaldehyde for 15 min at room temperature, washed and stored in DPBS solution until staining. The fixed cells were stained and imaged, as described in the previous section.

2.8. Statistical Analysis

The data shown represent the mean ± standard mean error of 3 experimental replicates unless otherwise mentioned. Statistical analysis was performed by using analysis of variance (ANOVA) followed by the Bonferroni post hoc test.

3. Results and Discussion

3.1. Surface properties of plasma polymer coatings change pre- and post-sterilization

The propensity of FEP to promote cell adhesion and expansion is limited by its hydrophobic and chemically inert surface. Here, we modified the surface properties of FEP using PECVD for cell culture applications. O-rich and N-rich coatings were chosen to understand the effect of surface chemistry on hMSC adhesion. The PPCs were deposited from a mixture of hydrocarbon gas (ethylene) and heteroatom gases (ammonia/carbon dioxide). The hydrocarbon gas creates the carbonaceous polymer backbone, while the heteroatom introduces functional groups [25]. The elemental composition of the untreated and plasma polymers coated FEP surfaces were analyzed using XPS (Figure 1). The survey spectra of the FEP (untreated) shown in Figure 1 indicates the carbon (C1s) and fluorine (F1s) peaks at 285 eV and 689 eV, respectively. This shows the pristine

nature of the FEP polymer surface with carbon-fluorine bonds. Successful modification of FEP surfaces is observed through the appearance of oxygen (O1s, 532 eV) and nitrogen (N1s, 400 eV) peaks, and absence of fluorine peaks on the survey spectrum after PECVD treatment. This suggests the complete coverage of FEP surface with the plasma polymer layer. Based on XPS spectra, it is evident that the polymer layer consisting of ethylene-based polymer backbone with functional groups consisting of oxygen and nitrogen moieties has been deposited on FEP surfaces.

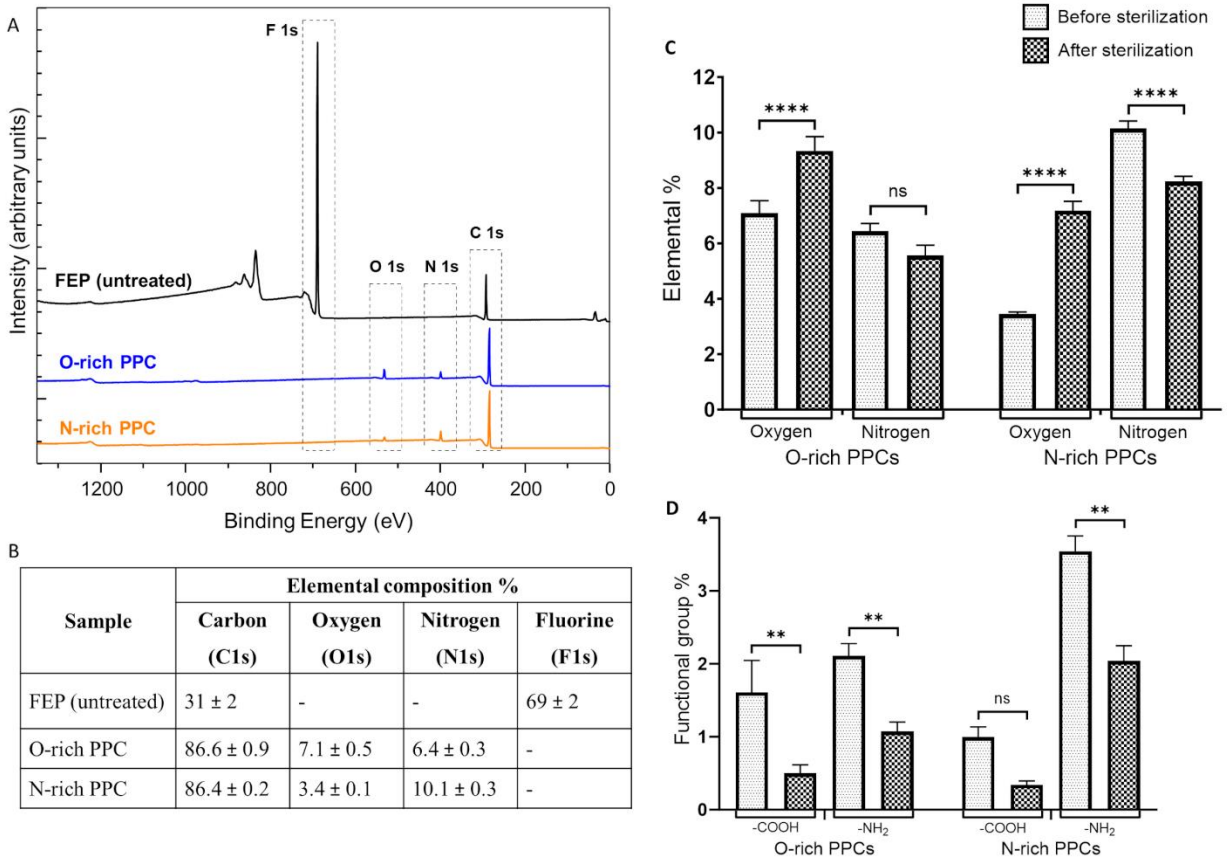

B

Sample	Elemental composition %			
	Carbon (C1s)	Oxygen (O1s)	Nitrogen (N1s)	Fluorine (F1s)
FEP (untreated)	31 ± 2	-	-	69 ± 2
O-rich PPC	86.6 ± 0.9	7.1 ± 0.5	6.4 ± 0.3	-
N-rich PPC	86.4 ± 0.2	3.4 ± 0.1	10.1 ± 0.3	-

Figure 1. Characterization of surface chemical composition. (A) XPS survey spectra and (B) elemental composition, C) Percentage of oxygen (O1s) and nitrogen (N1s) and (D) percentage of carboxylic acid (-COOH) and amines ($-NH_2$) functional groups, measured on O-rich PPC, and N-rich PPC surfaces before and after sterilization process. The -COOH and $-NH_2$ percentages were obtained after chemical derivatization process.

One crucial aspect to consider during plasma treatment for biological applications is the ability of the modified surfaces to retain their properties after the sterilization process. In surface engineering of materials, the process of sterilization can significantly impact plasma-modified surface properties [32]. The elemental composition observed via XPS (Figure 1B) revealed that the polymer coatings were composed of carbon, oxygen, and nitrogen with compositions related to the PECVD gas flow ratios (Table 1), as expected. Even though the sterilization process altered the elemental percentage, surfaces that were initially O-rich or N-rich maintained their overall bias towards higher oxygen or nitrogen content (Figure 1C). The reduction of nitrogen content was accompanied by an increase in oxygen content on both the O-rich and N-rich PPCs. This can be attributed to the surface oxidation and hydrolysis reaction occurring during the steam sterilization process [33].

In the context of biomaterials and medical device applications, the most extensively investigated chemical groups are carboxylic acid and amine surface functionalities. The carboxylic and amine functional groups can bind or interact with biological macromolecules [34, 35]. Figure 1D shows the changes in surface functional groups after the sterilization process. A decrease in both the carboxylic and amine surface functionalities was observed. The surface oxidation might have converted amines into other nitrogen functionalities such as imines, nitrile, and amides resulting in a decrease in the amine percentage. Also, the ionic interaction between the carboxylic and amine functionalities during the steam sterilization process might have reduced the overall percentage of the measured functional groups available on the surface.

Plasma-modified surfaces developed using non-polymerizing gases undergo aging processes reaching an eventual equilibrium. Generally, the functionalized plasma polymer coatings exhibit minimal aging effects due to the protective branched, cross-linked plasma polymer network [36].

Therefore, we examined the stability of O-rich and N-rich PPCs under different storage conditions for short- and long-term effects. Both O-rich and N-rich PPCs showed a statistically significant increase in oxygen % stored in an air environment (Figure 2A and B). The increase in oxygen % before sterilization is likely attributed to structural reorganization to minimize surface energy. This typically occurs during the initial few days after deposition, until day 7 and then stabilizes afterward [37]. However, sterilized O-rich and N-rich PPC surfaces oxidized in air environment compared to inert storage condition in argon environment. Oxidation of the organic polymer matrix is a known phenomenon, where radicals and loosely bound oligomeric structures trapped in the matrix undergo chemical reactions with atmospheric oxygen [38]. The oxygen % on day 5 and day 7 indicates that the surfaces begin to stabilize. Notably, nitrogen % for both PPCs remained unchanged after sterilization in both storage conditions over time, demonstrating the stability of nitrogen moieties on the modified surfaces.

Surface wettability significantly impacts protein adsorption and cell adhesion on materials. Water contact angles were measured on PPCs before and after steam sterilization were studied over different days to understand the wettability properties**Figure 2**. FEP (untreated) is a hydrophobic polymer with a water contact angle of 107 ± 2°. The introduction of O-rich and N-rich PPCs significantly decreased the contact angle to 67 ± 1° and 68 ± 1°, respectively. Despite changes in surface chemistry observed with XPS studies after sterilization, no significant differences were observed before and after sterilization or under different storage conditions (air or inert atmosphere) up to a week post-treatment. Overall, PPCs exhibit stability under inert conditions while maintaining their surface chemistry and wettability.

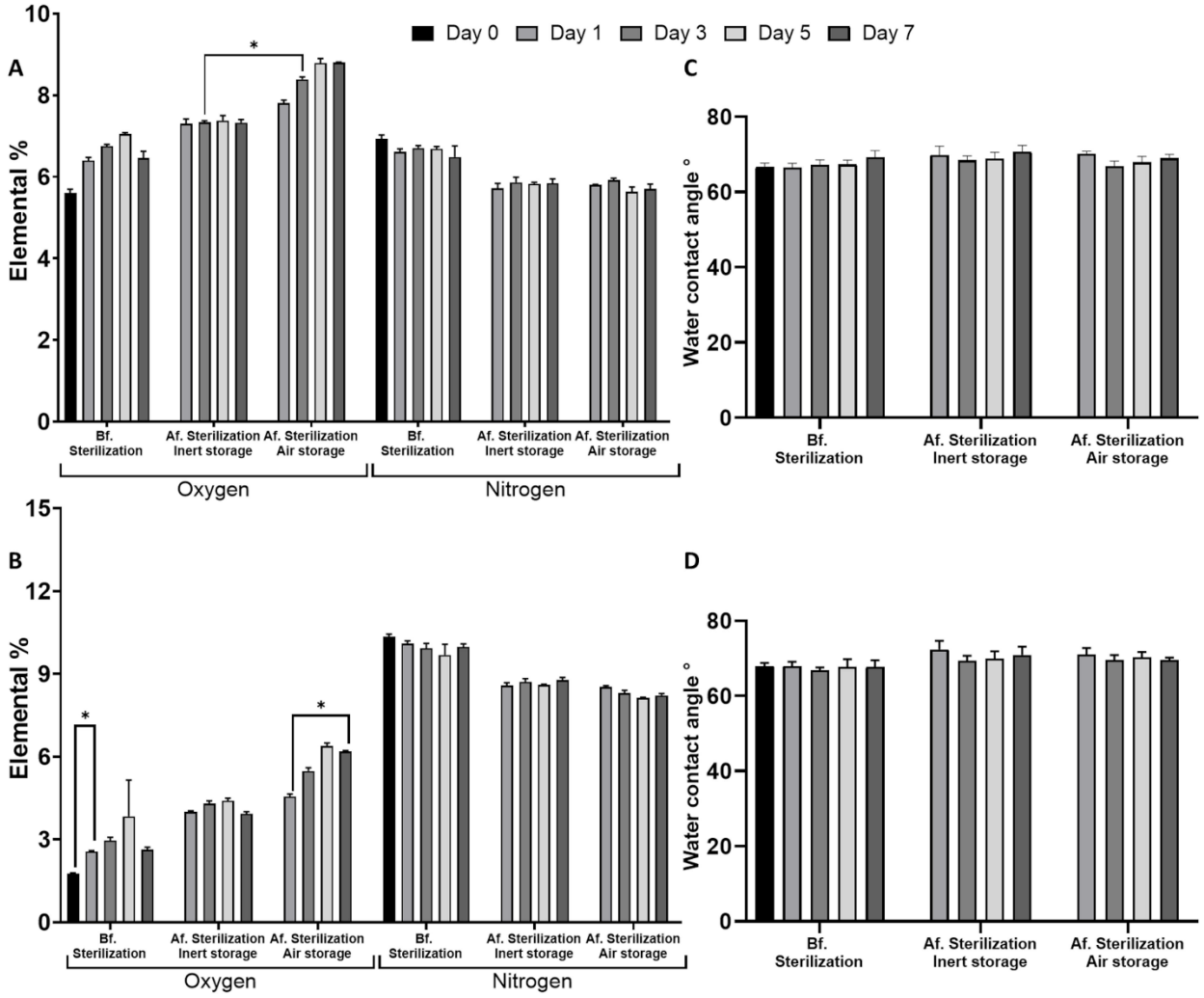

Figure 2. Coating stability was measured through XPS for (A) O-rich PPCs and (B) N-rich PPCs before (Bf.) and after (Af.) sterilization under different aging conditions (Day 0,1,3,5,7). [Note: The elemental % of O-rich PPCs and N-rich PPCs before sterilization showed statistical significance compared to both storage conditions after sterilization, as indicated in Figure 1].

Surface topography can affect cell adhesion, morphology and fate decisions depending on the scale of features present and cell-intrinsic factors [39, 40]. FEP surface topography and roughness were analyzed via AFM with and without PPC surface modification and sterilization. The AFM profiles (Figure 3) demonstrated that plasma polymer deposition modified FEP nanoscale features on the surfaces while retaining microscale crevasses formed during the FEP fabrication process.

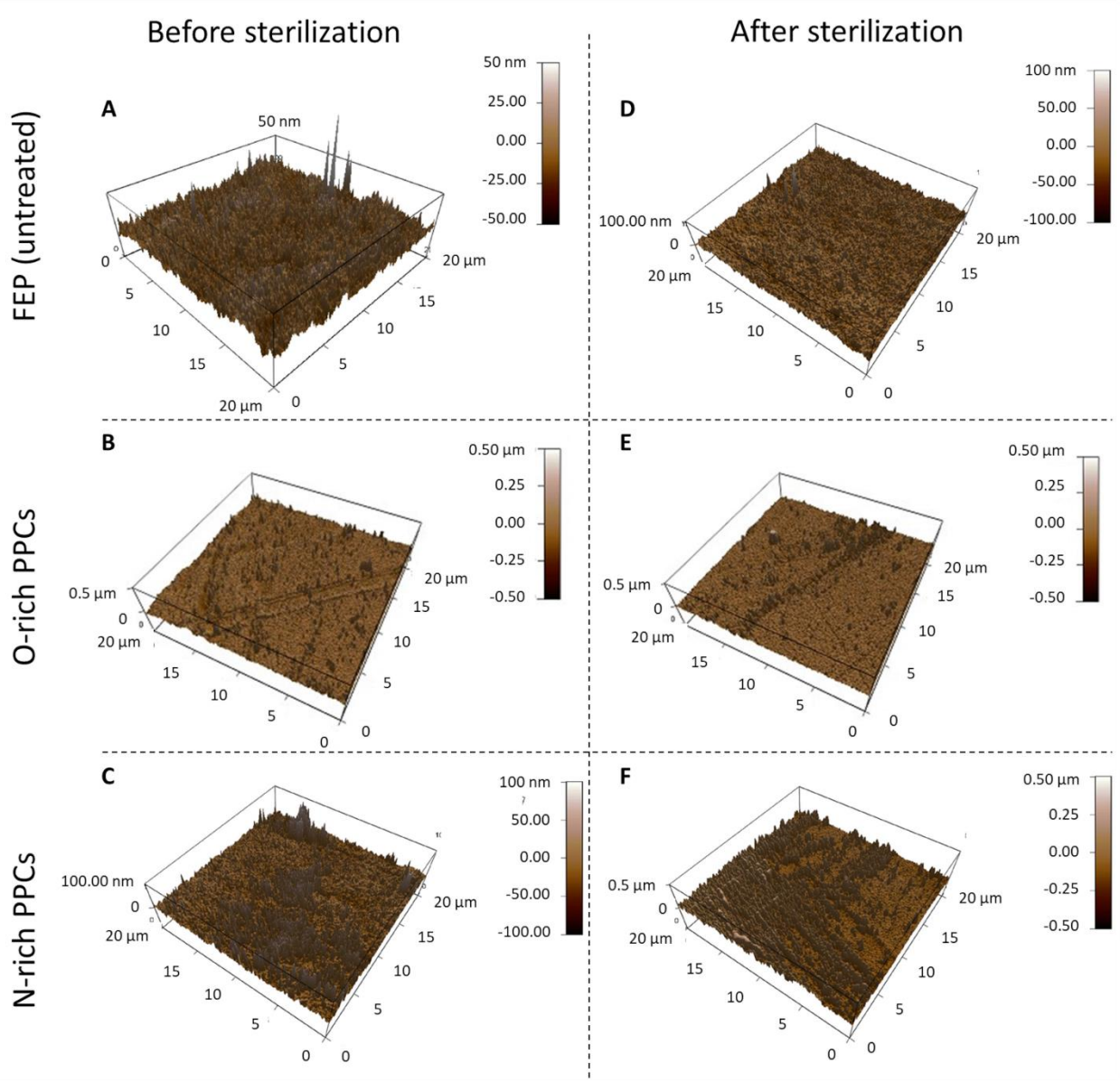

Figure 3. AFM 3D profiles of FEP surfaces before (A-C) and after (D-E) steam sterilization. (A, D) Untreated FEP; (B, E) coated with O-rich PPCs; (C, F) coated with N-rich PPCs.

The root means square roughness (Rq) of FEP (untreated), O-rich PPC, and N-rich PPC surfaces was 7.9 ± 0.5, 10 ± 2, 31 ± 8 nm, respectively. The surface roughness increased after steam sterilization for FEP (untreated) and N-rich PPC treated surfaces shown in supplementary information (Table S1.1). The initial topography on the FEP film, described as valleys formed during its fabrication, may result in local stress concentration within the plasma polymer layer

after deposition. Higher stress relief may occur at the edge of these valleys during sterilization and form local nodules, which led to an increase in surface roughness [41]. It was observed that the nodules on O-rich surfaces were lower than those on N-rich surfaces, resulting in mild effects from sterilization.

3.2. Increased amounts of adsorbed albumin observed via QCM-D

Upon cell seeding, proteins present in the medium rapidly adsorb to form complex adlayers that affect cell adhesion mechanism [42]. Albumin is an essential component of the cell culture medium and constitutes about 60% of the total protein in serum [43]. Hence, human serum albumin (HSA) was chosen as a model protein for protein adsorption studies using QCM-D analysis. PP 20:10:10 was selected as a model surface for O-rich and N-rich PPC surfaces in the QCM-D experiment. In aqueous conditions, the N-rich surfaces undergo oxidation and hydrolysis reactions, resulting in increased oxygen content forming an O-rich surface [44]. Here, PP 20:10:10 is a N-rich surface (N% = 10.9% ± 0.6%, O% = 6.2% ± 0.4%), which turns to an O-rich surface (N% = 8.7% ± 0.3%, O% = 11.3% ± 0.4%) after 24 h in PBS. However, it should not be misunderstood that N-rich surfaces always transition to O-rich surfaces under cell culture conditions. In cell culture settings, initial rapid protein adsorption occurs within the first 15 min, followed by cell adhesion to the reactive surfaces [45, 46]. Therefore, the conversion of N-rich surfaces to O-rich surfaces, which typically occurs after 24 h in an aqueous medium, will be more limited. This is because a multilayer of proteins has already bound to the functionalized surfaces, followed by cell adhesion.

Figure 4 shows the frequency and dissipation profiles for HSA adsorption on O-rich and N-rich PPC surfaces. The frequency change results from the protein ad-layer depositing on the plasma-coated surfaces. For N-rich surfaces, immediate adsorption of albumin is observed compared to O-rich PPCs. Compared to the previously reported frequency change of albumin adsorption on

untreated fluoropolymer (Δf = -10 Hz) [46], both the N-rich PPCs (Δf = -142.8 Hz) and O-rich PPCs surfaces (Δf = -62 Hz) showed increased shift. This suggests that the plasma polymer-coated surfaces have increased protein adsorption compared to untreated fluoropolymer, with N-rich PPCs showing the maximum albumin adsorption. As the isoelectric point of albumin is ~4.9 (overall negative charge of the protein at pH 7.4), protonated amine groups formed in PBS could immediately form ionic interactions with HSA chains on the surface. The positive charge of the surface amine functional groups binds electrostatically to the negatively charged proteins and cells at physiological pH [47]. The carboxylic groups in their negative ionic state are less prone to albumin adsorption than amine-rich surfaces.

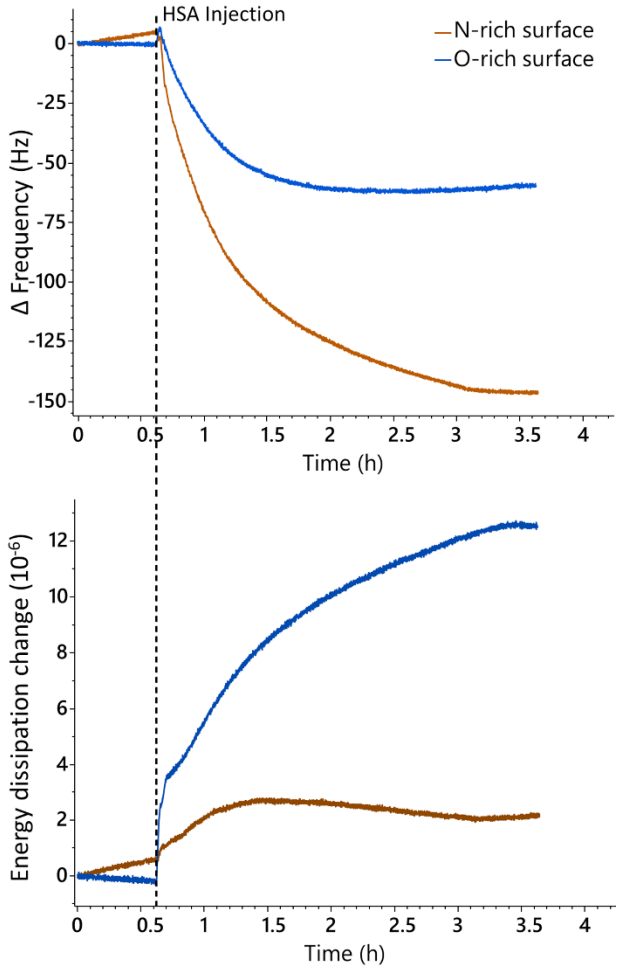

Figure 4. QCM-D profile of the human serum albumin adsorption kinetics on O-rich and N-rich PPC surfaces.

The change in the energy dissipation corresponds to the non-rigidity of the protein adlayers deposited on the surfaces. The energy dissipation is constant after 2 h on the N-rich PPC surface. Conversely, the energy dissipation continues to increase after 2 h on the O-rich PPC surface. This observation indicates that the HSA layer tends to be more rigid on the N-rich PPC compared to O-rich PPCs. Being in a protonated state because of amine functional groups, the N-rich PPC surface could bind firmly to the negatively charged albumin in PBS. However, the carboxylic functional

groups bind to the albumin more flexibly by hydrogen bonds. Surface functional groups play an essential role in the conformation of the protein adsorption, thereby affecting cell adhesion [48].

3.3. Initial hMSC adhesion is integrin-dependent in the presence of proteins but more dependent on PPC chemistry in the absence of proteins

Initial hMSC adhesion mechanisms were explored by culturing the hMSCs in protein-containing and protein-free media, with or without EDTA as a chelator (Figure 5). Integrins, an important cell surface receptor, are responsible for the initial cell attachment and spreading through adsorbed proteins [49]. Divalent cations such as Ca^{2+}, Mn^{2+} and Mg^{2+} bind to cation-binding sites of integrins, which in turn regulates integrin binding affinity with specific targets. The addition of EDTA, a chelating agent which sequesters divalent cations, diminishes the ability of cells to bind to the surface through this mechanism [50].

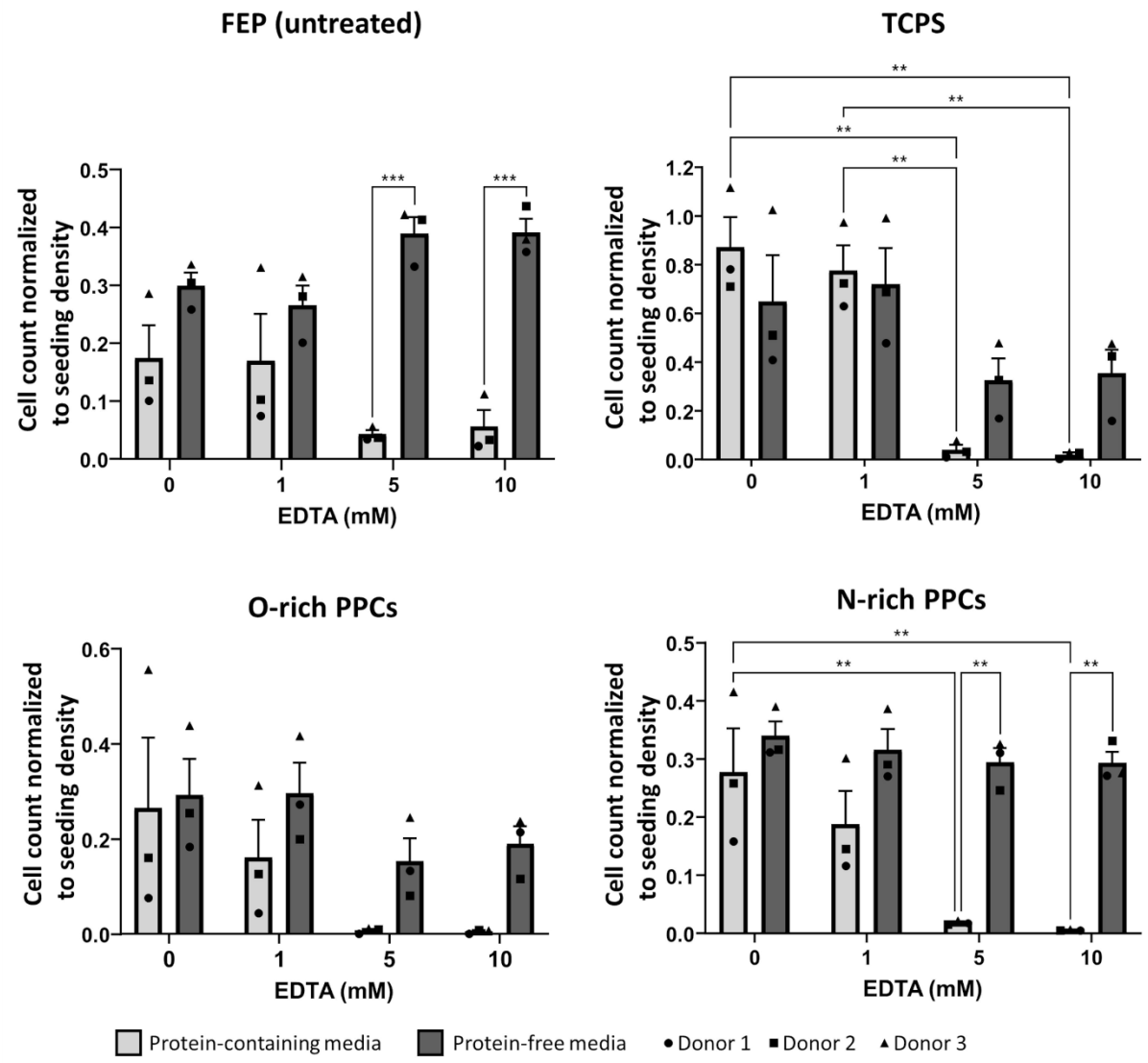

Figure 5. Inhibitory effect of EDTA on hMSCs cultured on different surfaces in protein-containing and protein-free media for 1 h. *p<0.5, **p<0.1, ***p<0.001.

As shown in Figure 5, a broad trend of decreasing numbers of adhered hMSCs with increasing concentration of EDTA was observed on all surfaces in protein-containing medium. At 5 to 10 mM EDTA, hMSC adhesion was nearly abrogated when proteins were present. Conversely, significant levels of hMSC adhesion were observed in protein-free medium, even in the presence of 10 mM EDTA. Perhaps most surprisingly, on FEP (untreated), nearly half of the hMSCs seeded adhered to surfaces after 1 h even with 10 mM EDTA. These results imply that integrin-

independent mechanisms can lead to significant hMSC tethering to surfaces in the absence of proteins – including electrostatic interactions in the case of the O-rich and N-rich surfaces, and the hydrophobic effect in the case of FEP (untreated). In the presence of proteins, FEP surfaces become shielded by proteins which mediate hMSC adhesion at least in part via integrins. The conformation taken by these proteins (e.g., unfolding more likely on untreated FEP than PPCs) may then significantly impact cell adhesion propensity [51, 52].

These results support the notion that in protein-containing media, initial cell adhesion events are almost exclusively governed by integrins binding to proteins (Figure 6). The action of protein adsorption on the material surface is driven by a tendency to increase the system's overall entropy and cause a concomitant decrease in the free energy of the surface [53]. In the presence of EDTA, integrin-mediated binding is prevented, and therefore cells cannot interact with the adsorbed protein layer. As a result, the adsorbed layer acts as a surfactant as it blocks the cells from any interactions with the underlying surface. On the other hand, the cells in the protein-free media tend to adhere to different surfaces based on their surface properties (i.e., surface chemistry, roughness, and wettability). Combining the QCM-D results with this assay suggests that rapid and higher protein adsorption on the N-rich PPCs compared to O-rich PPCs may be the reason for the changes in the initial cell attached observed between the PPCs. Hoshiba *et al.* reported a similar phenomenon about the charged polymers influencing the adhesion mechanism of human fibrosarcoma and human cervix epithelioid carcinoma cells [54]. The cell-material interactions explored in the study were hydrophobic, electrostatic and biological adhesion. Hence, understanding the effect of PPC's surface properties on the mechanism of cell adhesion will help to tune their properties for the desired application.

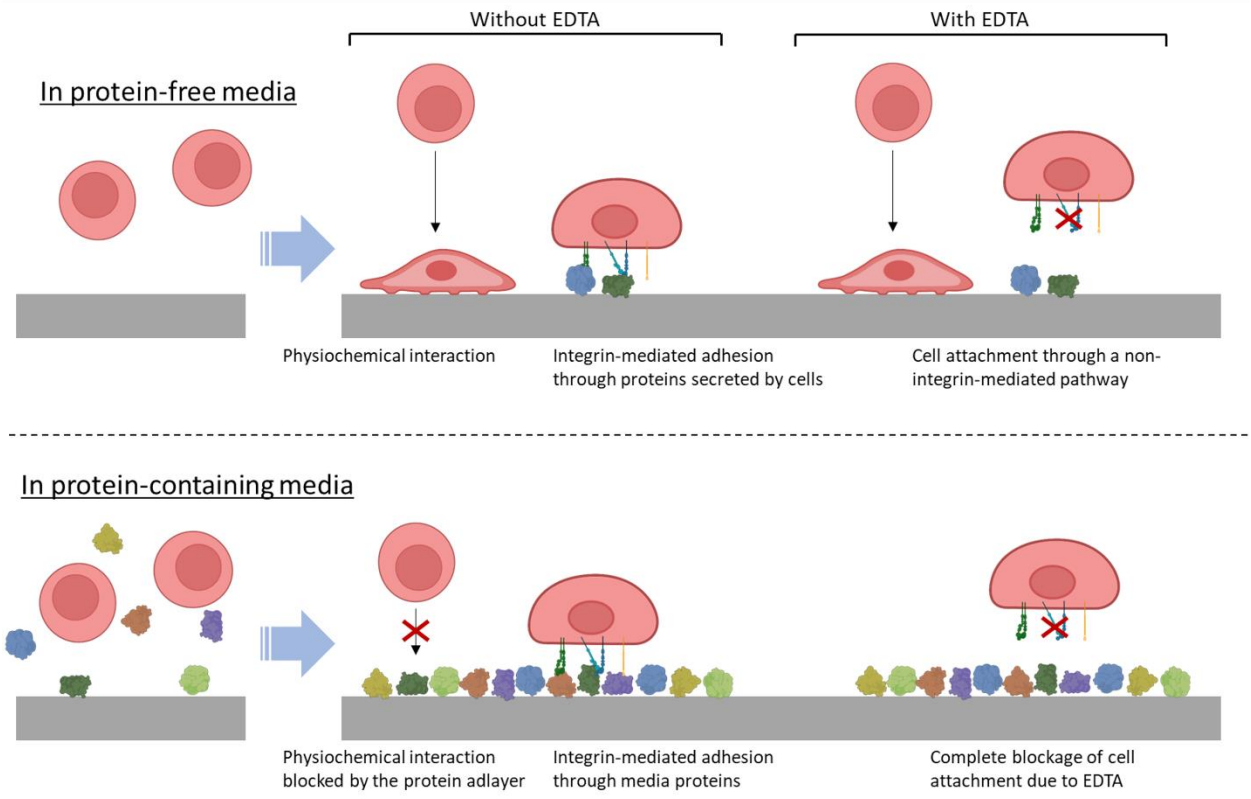

Figure 6. Schematic of proposed hMSC adhesion mechanisms in protein-containing and protein-free media. Created with BioRender.com

3.4. N-rich plasma polymer coated FEP surfaces match the performance of conventional TCPS for hMSC adhesion and expansion

hMSCs were cultured in StemMACS™ MSC expansion medium for up to 3 days to determine the effect of the different plasma polymer-coated surfaces on cell adhesion and expansion (Figure 7A). At day 1, hMSCs adhered well on both the O-rich and N-rich PPCs with cell numbers matching the seeding density, whereas low yields were observed on FEP (untreated). At day 3, compared with FEP (untreated) surfaces, all the other surfaces showed a statistically significant increase in cell adhesion and expansion. Among the functionalized surfaces, the highest hMSC expansion (~7-fold) was observed on the N-rich PPCs, followed by TCPS (~6-fold) and then O-rich PPCs (~3-fold).

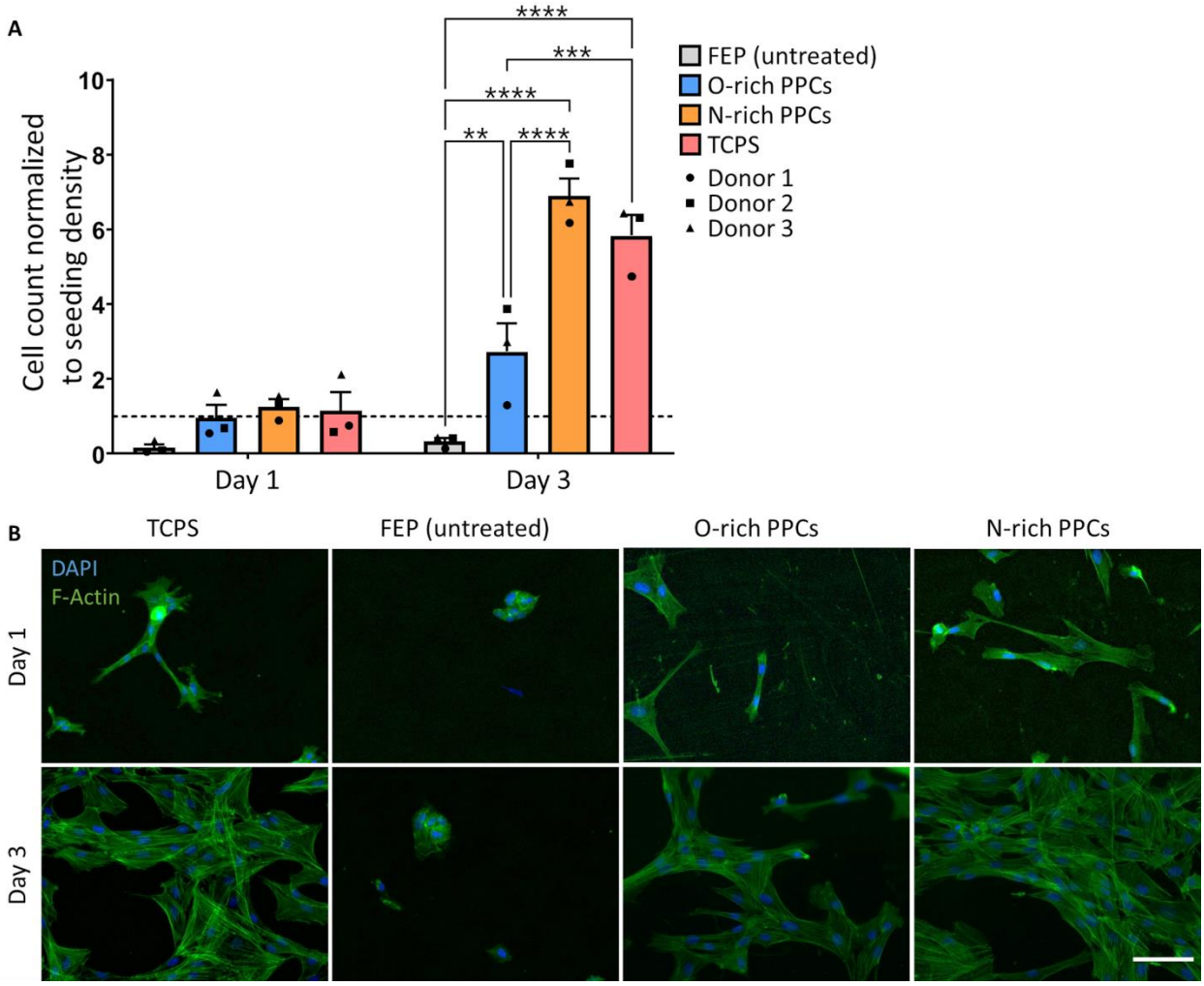

Figure 7. hMSC expansion and morphology on plasma polymer coated FEP and controls. (A) Cell nuclei count for hMSCs cultured on FEP (untreated), O-rich PPCs, N-rich-PPCs, TCPS, after day 1 and day 3. Seeding density = 5,000 cells/cm^2. (B) Adhered hMSC morphology. Cells were stained with DAPI (blue) and phalloidin (filamentous actin, green). Scale bar is 100 µm.

The physicochemical properties of materials, such as surface chemistry, wettability, and roughness influence the cell-material interaction [55]. Using the PECVD technique, these properties are modified on the FEP surfaces to have a combined effect for improving the hMSC adhesion and expansion over the pristine polymer. In general, the cell adhesion process involves two phases: a short early phase for the attachment of the cells through physicochemical linkage

and a later phase involving the adhesion and spreading of cells through the various proteins in the environment [56]. During the early phase, the plasma-deposited coatings increased the cell adhesion compared to hydrophobic FEP (untreated), while little difference emerged between the O-rich and N-rich PPCs. A significant difference between the O-rich and N-rich PPCs emerged after 3 days of growth, where PPC surface chemistry and adsorbed proteins may bear more influence. This is consistent with previously reported studies, showing that the aminated surfaces have higher cell adhesion compared to carboxylated and hydroxylated surfaces [34, 57]. The positive charge of the surface amine functional groups binds electrostatically to the negatively charged proteins and cells at physiological pH [47].

The cell spreading on the surfaces was assessed by labelling filamentous actin in the cell cytoskeleton (Figure 7B). Only a few adherent cells were observed on the FEP (untreated) surface, and those present tended to aggregate. This is mainly due to the repelling nature of the hydrophobic inert FEP (untreated). In contrast, hMSCs on O-PPCs and N-PPCs on day 1 displayed a spindle-shaped population with spread-out, distinct actin filaments. On day 3, more confluent and well-spread cells were observed across the plasma polymer-coated FEP and control TCPS surfaces. The cell morphology corroborated the expansion profile confirming that cells attach more efficiently onto the functionalized PPC surfaces. The surface functional groups such as -NH_2, -COOH, and -OH assists the adhesion of cell culture media proteins such as vitronectin and fibronectin from the cell culture media [58]. The adhesion of aforementioned proteins varies based on the complex media, whose compositions are not disclosed due to proprietary reasons. Besides the culture media, the extracellular proteins secreted by the cells tend to regulate the cell adhesion and affects the cytoskeleton [59]. The integrin-binding motifs in these extracellular matrix proteins mediate cell adhesion and spreading [60].

One of the critical requirements for developing a new expansion culture vessel is that surface modification strategies should not affect the hMSC phenotype. Flow cytometry analysis was employed to identify the immunophenotypic profile of the expanded hMSCs. hMSCs were characterized using a panel of surface markers in accordance with the guidelines provided by the International Society for Cell & Gene Therapy. Accordingly, hMSCs should exhibit expression of CD105, CD73, and CD90, while lacking expression of CD45, CD34, CD14 or CD11b, CD79α or CD19, and HLA-DR surface molecules [31]. These markers The surface marker expression by the hMSCs on different surfaces on day 3 was listed in Supplementary information (Table S1.2). Low hMSC yield on FEP (untreated) did not permit reliable hMSC surface marker profiling. hMSCs cultured in both the O-rich and N-rich PPC surfaces expressed similar phenotypic markers as hMSCs cultured on TCPS, except for the higher CD34 marker expression. CD34 is generally considered a hematopoietic stem cell and endothelial cell marker [61], however, the existence of a positive CD34 hMSC subpopulation was identified and discussed in the literature [62, 63]. The possibility of functional groups on PPCs affecting the lineage of hMSC needs to be explored. While assessing the differentiation potential of the hMSCs was outside the scope of this work, studies have shown that surfaces with different functional groups can direct the differentiation of the MSC towards the osteogenic or chondrogenic lineages [64, 65]. It would be interesting to develop PPC compositions tailored to desired hMSC differentiation fates within closed culture systems.

4. Impact and Future Directions

Versatile cell culture systems adapted to clinical-grade manufacturing of anchorage-dependent cells such as hMSCs are in growing demand [66, 67]. Current strategies for manufacturing MSCs involve various types of culturing systems such as multilayered cell flasks, roller bottles, stirred

bioreactors, hollow-fiber bioreactors, and fixed-bed bioreactors [68]. Ready-to-use disposable plasma polymer-coated FEP bags can be added as a valuable contender to these existing culture vessels as a cGMP complaint closed system; especially for the expansion of autologous MSCs, which require smaller vessel sizes with cost-effective bioprocess design in the clinical settings [69]. PECVD is one such surface modification technique that can be used to achieve the desired biological outcomes in developing new biomedical devices [70, 71]. In this study, thin films with carboxylic and amine functional groups were successfully applied to FEP surfaces with surface chemistry easily modulated through the gas flow ratio applied in PECVD.

A key consideration when implementing novel coatings for cell culture, particularly towards clinical applications, is stability under sterilization conditions compatible with regulatory requirements. The O-rich and N-rich PPCs developed in this study did not delaminate nor undergo excessive chemical changes (i.e., they respectively remain O-rich and N-rich) under conditions applied in industry for sterilization of fluoropolymer cell culture bags. Additionally, the stability studies revealed that the surfaces maintained their chemistry and wettability in storage under inert atmosphere for both short- and long-term applications. It is also recommended to seal the surfaces in low oxygen-permeable bags under inert conditions, as this approach ensures their stability for long-term applications. Furthermore, this process is feasible for translating these coatings into a closed-bag system. The increased surface roughness at the nanometer-scale and shift in surface chemistry can be characterized and integrated into process knowledge. The resulting sterilized functionalized FEP surfaces were effective in expanding hMSCs, with N-rich PPC treated FEP on par with TCPS surfaces based on 1-day cell adhesion, 3-day cell expansion, hMSC morphology and surface marker profiling.

From a materials perspective, cell adhesion depends on various surface properties such as surface chemistry, wettability, charge, roughness, and free energy. Besides these properties, the environmental conditions such as temperature, pH, proteins, and small molecules present in the media are also implicated in the cell-material interaction. In particular, prior adsorption of proteins on the material surface imposes a profound effect on cell adhesion. Integrins and other cell receptors recognize and bind to particular sequences present within surface-adsorbed proteins such as fibronectin, vitronectin, and laminin, promoting cell adhesion [72]. Thus, regulating protein adsorption ultimately controls cell adhesion. QCM-D showed that N-rich PPCs favored protein adsorption compared to O-rich PPCs, thus resulting in higher protein-mediated cell adhesion and expansion. The literature also shows that cell adhesion is favored on positively charged surfaces rather than negatively charged ones [55]. The initial cell adhesion studies using the chelator showed the different cell adhesion mechanisms in protein-free and protein-containing media. Hence, the cell adhesion pathway on PPCs may possibly be controlled in the future by understanding its mechanism. This study advances our technical understanding of depositing O-rich and N-rich PPCs on FEP bags, which can be leveraged for biomanufacturing of hMSCs in sterilizable culture vessels in clinical settings.

5. Conclusion

The surface properties of the material play a pivotal role in the outcome of the success of any biomedical device. Understanding the cell-material interaction will help in the culturing process of anchorage-dependent cell therapy products such as hMSCs. In this study, we showed that plasma deposition by three gas mixtures (ethylene/carbon dioxide/ammonia) could be tailored to develop O-rich and N-rich plasma polymer coatings on FEP surfaces. Steam sterilization, a crucial step in the use of materials in clinical practice, affects the surface chemistry, wettability, and

roughness of these plasma polymer coatings. Post-sterilization, these coatings maintained their overall attributes as O-rich or N-rich coatings with high surface wettability. It was found that the stability of these coatings was better in an inert argon environment compared to storage in the air environment. Further exploration using QCM-D studies showed that albumin adsorbed more rigidly and faster on N-rich surfaces than on O-rich surfaces. The physicochemical properties of these plasma surfaces combined with the adsorption of media-derived proteins significantly impacted the adhesion behavior of hMSCs on modified FEP surfaces. Despite both plasma-treated surfaces showing increased hMSC adhesion and expansion compared with unmodified FEP, the N-rich surfaces are more favorable and comparable with commercial TCPS surfaces. Plasma polymer coatings could be applied to FEP bags and other cell culture systems to aid in the biomanufacturing of anchorage-dependent cell therapy products such as hMSCs.

Author contributions

CReDIT roles are as follows:

B.R.: Methodology; Data curation; Formal analysis; Investigation; Validation; Visualization; Software; Writing - Original Draft; Writing - review & editing.

G.S.: Conceptualization; Methodology; Data curation; Formal analysis; Investigation; Validation; Writing - Original Draft; Writing - review & editing.

O.B: Investigation; Formal analysis; Writing - review & editing.

K.C.: Resources, Project administration; Writing - review & editing.

N.F.: Funding acquisition; Resources, Project administration; Writing - review & editing.

PLGL. and C.H.: Supervision; Resources; Funding acquisition; Project administration; Conceptualization; Methodology; Validation; Writing - review & editing.

Acknowledgment

We thank Michel L. Tremblay, Rachel Pytel, Nabil Zeidan, and Jessica Tian for their insightful comments. This work was undertaken, in part, thanks to funding from the Canada Research Chairs program (C.H.). We also thank the following networks for activities in support of this project: Quebec Cell, Tissue and Gene Therapy Network–ThéCell (a thematic network supported by the Fonds de recherche du Québec–Santé); PROTEO (The Quebec Network for Research on Protein Function), CQMF/QCAM (Quebec Centre for Advanced Materials); Canada's SCN (Stem Cell Network).

Funding

This project is funded to McGill University through Collaborative Research and Development (CRD) Grant between Saint-Gobain Ceramics & Plastics, Inc., Canada's National Sciences and Engineering Research Council Collaborative Research and Development Grants [CRDPJ/533984-2018], MEDTEQ - a Quebec Consortium for Industrial Research and Innovation in Medical Technology [11-C Thérapie Cellulaire] and MITACS [IT16899 ACC]. These funds supported all the work in this project and were used to pay trainee stipends, consumables, and small equipment.

REFERENCES

[1] L.L.-W. Wang, M.E. Janes, N. Kumbhojkar, N. Kapate, J.R. Clegg, S. Prakash, M.K. Heavey, Z. Zhao, A.C. Anselmo, S. Mitragotri, Cell therapies in the clinic, Bioengineering & Translational Medicine 6(2) (2021) e10214.

[2] V. Jossen, C. van den Bos, R. Eibl, D. Eibl, Manufacturing human mesenchymal stem cells at clinical scale: process and regulatory challenges, Applied Microbiology and Biotechnology 102(9) (2018) 3981-3994.
[3] P. Jayaraman, R. Lim, J. Ng, M.C. Vemuri, Acceleration of Translational Mesenchymal Stromal Cell Therapy Through Consistent Quality GMP Manufacturing, Frontiers in Cell and Developmental Biology 9(636) (2021).
[4] V.F. Cardoso, D.M. Correia, C. Ribeiro, M.M. Fernandes, S. Lanceros-Méndez, Fluorinated Polymers as Smart Materials for Advanced Biomedical Applications, Polymers (Basel) 10(2) (2018) 161.
[5] N. Fekete, A.V. Béland, K. Campbell, S.L. Clark, C.A. Hoesli, Bags versus flasks: a comparison of cell culture systems for the production of dendritic cell–based immunotherapies, Transfusion 58(7) (2018) 1800-1813.
[6] K. Menck, D. Behme, M. Pantke, N. Reiling, C. Binder, T. Pukrop, F. Klemm, Isolation of human monocytes by double gradient centrifugation and their differentiation to macrophages in teflon-coated cell culture bags, J Vis Exp (91) (2014) e51554-e51554.
[7] J.-P. Bastien, N. Fekete, A.V. Beland, M.-P. Lachambre, V. Laforte, D. Juncker, V. Dave, D.-C. Roy, C.A. Hoesli, Closing the system: production of viral antigen-presenting dendritic cells eliciting specific CD8+ T cell activation in fluorinated ethylene propylene cell culture bags, Journal of Translational Medicine 18(1) (2020) 383.
[8] D. Gulen, F. Abe, S. Maas, E. Reed, K. Cowan, S. Pirruccello, J. Wisecarver, P. Warkentin, M. Northam, O. Turken, U. Coskun, J. Senesac, J.E. Talmadge, Closing the manufacturing process of dendritic cell vaccines transduced with adenovirus vectors, International Immunopharmacology 8(13) (2008) 1728-1736.
[9] A. Mizukami, K. Swiech, Platforms for Clinical-Grade CAR-T Cell Expansion, in: K. Swiech, K.C.R. Malmegrim, V. Picanço-Castro (Eds.), Chimeric Antigen Receptor T Cells: Development and Production, Springer US, New York, NY, 2020, pp. 139-150.
[10] M. Abou-El-Enein, M. Elsallab, S.A. Feldman, A.D. Fesnak, H.E. Heslop, P. Marks, B.G. Till, G. Bauer, B. Savoldo, Scalable Manufacturing of CAR T cells for Cancer Immunotherapy, Blood Cancer Discov 2(5) (2021) 408-422.
[11] J. Kadarusman, R. Bhatia, J. McLaughlin, W.R. Lin, Growing Cholesterol-Dependent NS0 Myeloma Cell Line in the Wave Bioreactor System: Overcoming Cholesterol-Polymer Interaction by Using Pretreated Polymer or Inert Fluorinated Ethylene Propylene, Biotechnology Progress 21(4) (2005) 1341-1346.
[12] P.A. Gupta, X. Ge, Y. Kostov, G. Rao, A completely noninvasive method of dissolved oxygen monitoring in disposable small-scale cell culture vessels based on diffusion through permeable vessel walls, Biotechnology Progress 30(1) (2014) 172-177.
[13] I. Ullah, Raghavendra B. Subbarao, Gyu J. Rho, Human mesenchymal stem cells - current trends and future prospective, Bioscience Reports 35(2) (2015).
[14] N. Kim, S.-G. Cho, Clinical applications of mesenchymal stem cells, Korean J Intern Med 28(4) (2013) 387-402.
[15] Search of: mesenchymal Stem cells - Results on Map - ClinicalTrials.gov. https://classic.clinicaltrials.gov/ct2/results/map?term=mesenchymal+Stem+cells&map=. (Accessed 3rd July, 2023.
[16] FDA Accepts Mesoblast's Resubmission of the Biologic License Application for Remestemcel-L In Children with Steroid-Refractory Acute Graft Versus Host Disease as a

Complete Response and Sets Goal Date of August 2, 2023, 2023. https://investorsmedia.mesoblast.com/static-files/d4c97ce2-fcba-4007-be6e-9d5e105a922a.
[17] M. Alvarez-Viejo, Y. Menendez-Menendez, M.A. Blanco-Gelaz, A. Ferrero-Gutierrez, M.A. Fernandez-Rodriguez, J. Gala, J. Otero-Hernandez, Quantifying Mesenchymal Stem Cells in the Mononuclear Cell Fraction of Bone Marrow Samples Obtained for Cell Therapy, Transplantation Proceedings 45(1) (2013) 434-439.
[18] VueLife® "AC" Series Bags. https://www.biopharm.saint-gobain.com/cell-therapy/vuelife-ac-series-bags.
[19] P. Liu, G. Wang, Q. Ruan, K. Tang, P.K. Chu, Plasma-activated interfaces for biomedical engineering, Bioactive Materials 6(7) (2021) 2134-2143.
[20] T. Desmet, R. Morent, N. De Geyter, C. Leys, E. Schacht, P. Dubruel, Nonthermal Plasma Technology as a Versatile Strategy for Polymeric Biomaterials Surface Modification: A Review, Biomacromolecules 10(9) (2009) 2351-2378.
[21] P.K. Chu, J.Y. Chen, L.P. Wang, N. Huang, Plasma-surface modification of biomaterials, Materials Science and Engineering: R: Reports 36(5) (2002) 143-206.
[22] T. Jacobs, R. Morent, N. De Geyter, P. Dubruel, C. Leys, Plasma Surface Modification of Biomedical Polymers: Influence on Cell-Material Interaction, Plasma Chemistry and Plasma Processing 32(5) (2012) 1039-1073.
[23] A. Artemenko, O. Kylián, A. Choukourov, I. Gordeev, M. Petr, M. Vandrovcová, O. Polonskyi, L. Bačáková, D. Slavinska, H. Biederman, Effect of sterilization procedures on properties of plasma polymers relevant to biomedical applications, Thin Solid Films 520(24) (2012) 7115-7124.
[24] R. Ghobeira, C. Philips, H. Declercq, P. Cools, N. De Geyter, R. Cornelissen, R. Morent, Effects of different sterilization methods on the physico-chemical and bioresponsive properties of plasma-treated polycaprolactone films, Biomed Mater 12(1) (2017) 015017.
[25] S. Babaei, P.-L. Girard-Lauriault, Tuning the Surface Properties of Oxygen-Rich and Nitrogen-Rich Plasma Polymers: Functional Groups and Surface Charge, Plasma Chemistry and Plasma Processing 36(2) (2016) 651-666.
[26] P.-L. Girard-Lauriault, P.M. Dietrich, T. Gross, T. Wirth, W.E.S. Unger, Chemical Characterization of the Long-Term Ageing of Nitrogen-Rich Plasma Polymer Films under Various Ambient Conditions, 10(4) (2013) 388-395.
[27] R. Michel, R. Luginbühl, D.J. Graham, B.D. Ratner, New Substrates for Polymer Cationization with Time-of-Flight Secondary Ion Mass Spectrometry, Langmuir 16(16) (2000) 6503-6509.
[28] C.-P. Klages, Z. Khosravi, A. Hinze, Some Remarks on Chemical Derivatization of Polymer Surfaces after Exposure to Nitrogen-Containing Plasmas, Plasma Processes and Polymers 10(4) (2013) 307-312.
[29] L.F. de Magalhães Brito, D. Magagna, Infection prevention & control—A clinical engineering perspective, in: E. Iadanza (Ed.), Clinical Engineering Handbook (Second Edition), Academic Press2020, pp. 682-693.
[30] Nunc Cell Culture Plastics and Cultureware. https://www.thermofisher.com/ca/en/home/life-science/cell-culture/cell-culture-plastics.html#surface-treatments.
[31] M. Dominici, K. Le Blanc, I. Mueller, I. Slaper-Cortenbach, F.C. Marini, D.S. Krause, R.J. Deans, A. Keating, D.J. Prockop, E.M. Horwitz, Minimal criteria for defining multipotent

mesenchymal stromal cells. The International Society for Cellular Therapy position statement, Cytotherapy 8(4) (2006) 315-317.
[32] M. Ahmed, G. Punshon, A. Darbyshire, A.M. Seifalian, Effects of sterilization treatments on bulk and surface properties of nanocomposite biomaterials, J Biomed Mater Res B Appl Biomater 101(7) (2013) 1182-1190.
[33] A. Simmons, J. Hyvarinen, L. Poole-Warren, The effect of sterilisation on a poly(dimethylsiloxane)/poly(hexamethylene oxide) mixed macrodiol-based polyurethane elastomer, Biomaterials 27(25) (2006) 4484-4497.
[34] Y. Arima, H. Iwata, Effects of surface functional groups on protein adsorption and subsequent cell adhesion using self-assembled monolayers, Journal of Materials Chemistry 17(38) (2007) 4079-4087.
[35] T.I. Croll, A.J. O'Connor, G.W. Stevens, J.J. Cooper-White, Controllable Surface Modification of Poly(lactic-co-glycolic acid) (PLGA) by Hydrolysis or Aminolysis I: Physical, Chemical, and Theoretical Aspects, Biomacromolecules 5(2) (2004) 463-473.
[36] M. Vandenbossche, D. Hegemann, Recent approaches to reduce aging phenomena in oxygen- and nitrogen-containing plasma polymer films: An overview, Current Opinion in Solid State and Materials Science 22(1) (2018) 26-38.
[37] P.-L. Girard-Lauriault, P.M. Dietrich, T. Gross, T. Wirth, W.E.S. Unger, Chemical Characterization of the Long-Term Ageing of Nitrogen-Rich Plasma Polymer Films under Various Ambient Conditions, Plasma Processes and Polymers 10(4) (2013) 388-395.
[38] P.-L. Girard-Lauriault, W.E.S. Unger, P.M. Dietrich, A. Holländer, Innovative and Established Strategies for the Surface Analysis of Nitrogen and Oxygen-Rich Plasma Polymer Films by XPS: An Introductory Guide, Plasma Processes and Polymers 12(9) (2015) 953-967.
[39] A.T. Nguyen, S.R. Sathe, E.K.F. Yim, From nano to micro: topographical scale and its impact on cell adhesion, morphology and contact guidance, Journal of Physics: Condensed Matter 28(18) (2016) 183001.
[40] Y. Hou, W. Xie, L. Yu, L.C. Camacho, C. Nie, M. Zhang, R. Haag, Q. Wei, Surface Roughness Gradients Reveal Topography-Specific Mechanosensitive Responses in Human Mesenchymal Stem Cells, Small 16(10) (2020) 1905422.
[41] M.Ö. Öteyaka, P. Chevallier, S. Turgeon, L. Robitaille, G. Laroche, Low Pressure Radio Frequency Ammonia Plasma Surface Modification on Poly(ethylene terephthalate) Films and Fibers: Effect of the Polymer Forming Process, Plasma Chemistry and Plasma Processing 32(1) (2012) 17-33.
[42] A. Hasan, S.K. Pattanayek, L.M. Pandey, Effect of Functional Groups of Self-Assembled Monolayers on Protein Adsorption and Initial Cell Adhesion, ACS Biomaterials Science & Engineering 4(9) (2018) 3224-3233.
[43] G.L. Francis, Albumin and mammalian cell culture: implications for biotechnology applications, Cytotechnology 62(1) (2010) 1-16.
[44] A. Contreras-García, M.R. Wertheimer, Low-Pressure Plasma Polymerization of Acetylene–Ammonia Mixtures for Biomedical Applications, Plasma Chemistry and Plasma Processing 33(1) (2013) 147-163.
[45] N. Recek, M. Jaganjac, M. Kolar, L. Milkovic, M. Mozetič, K. Stana-Kleinschek, A. Vesel, Protein Adsorption on Various Plasma-Treated Polyethylene Terephthalate Substrates, Molecules 18(10) (2013) 12441-12463.
[46] A. Wargenau, N. Fekete, A.V. Beland, G. Sabbatier, O.M. Bowden, M.D. Boulanger, C.A. Hoesli, Protein film formation on cell culture surfaces investigated by quartz crystal

microbalance with dissipation monitoring and atomic force microscopy, Colloids and Surfaces B: Biointerfaces 183 (2019) 110447.
[47] J.H. Lee, H.W. Jung, I.-K. Kang, H.B. Lee, Cell behaviour on polymer surfaces with different functional groups, Biomaterials 15(9) (1994) 705-711.
[48] K. Kushiro, C.-H. Lee, M. Takai, Simultaneous characterization of protein–material and cell–protein interactions using dynamic QCM-D analysis on SAM surfaces, Biomaterials Science 4(6) (2016) 989-997.
[49] J.M. Kang, T. Rajangam, J.W. Rhie, S.H. Kim, Characterization of cell signaling, morphology, and differentiation potential of human mesenchymal stem cells based on cell adhesion mechanism, J Cell Physiol 235(10) (2020) 6915-6928.
[50] K. Zhang, J. Chen, The regulation of integrin function by divalent cations, Cell Adhesion & Migration 6(1) (2012) 20-29.
[51] M.M. Ouberai, K. Xu, M.E. Welland, Effect of the interplay between protein and surface on the properties of adsorbed protein layers, Biomaterials 35(24) (2014) 6157-6163.
[52] A. Hasan, G. Waibhaw, L.M. Pandey, Conformational and Organizational Insights into Serum Proteins during Competitive Adsorption on Self-Assembled Monolayers, Langmuir 34(28) (2018) 8178-8194.
[53] E. Kaivosoja, G. Barreto, K. Levón, S. Virtanen, M. Ainola, Y.T. Konttinen, Chemical and physical properties of regenerative medicine materials controlling stem cell fate, Annals of Medicine 44(7) (2012) 635-650.
[54] T. Hoshiba, C. Yoshikawa, K. Sakakibara, Characterization of Initial Cell Adhesion on Charged Polymer Substrates in Serum-Containing and Serum-Free Media, Langmuir 34(13) (2018) 4043-4051.
[55] S. Cai, C. Wu, W. Yang, W. Liang, H. Yu, L. Liu, Recent advance in surface modification for regulating cell adhesion and behaviors, Nanotechnology Reviews 9(1) (2020) 971-989.
[56] K. Anselme, L. Ploux, A. Ponche, Cell/Material Interfaces: Influence of Surface Chemistry and Surface Topography on Cell Adhesion, Journal of Adhesion Science and Technology 24(5) (2010) 831-852.
[57] Y. Wang, Y. Ji, Y. Zhao, Y. Kong, M. Gao, Q. Feng, Y. Wu, Y. Yang, Effects of surface functional groups on proliferation and biofunction of Schwann cells, Journal of Biomaterials Applications 30(10) (2016) 1494-1504.
[58] Y. Arima, H. Iwata, Preferential adsorption of cell adhesive proteins from complex media on self-assembled monolayers and its effect on subsequent cell adhesion, Acta Biomaterialia 26 (2015) 72-81.
[59] B.K. Mann, A.T. Tsai, T. Scott-Burden, J.L. West, Modification of surfaces with cell adhesion peptides alters extracellular matrix deposition, Biomaterials 20(23) (1999) 2281-2286.
[60] N. Faucheux, R. Schweiss, K. Lützow, C. Werner, T. Groth, Self-assembled monolayers with different terminating groups as model substrates for cell adhesion studies, Biomaterials 25(14) (2004) 2721-2730.
[61] L. Fina, H.V. Molgaard, D. Robertson, N.J. Bradley, P. Monaghan, D. Delia, D.R. Sutherland, M.A. Baker, M.F. Greaves, Expression of the CD34 Gene in Vascular Endothelial Cells, Blood 75(12) (1990) 2417-2426.
[62] C.-S. Lin, H. Ning, G. Lin, T.F. Lue, Is CD34 truly a negative marker for mesenchymal stromal cells?, Cytotherapy 14(10) (2012) 1159-1163.

[63] S. Kaiser, B. Hackanson, M. Follo, A. Mehlhorn, K. Geiger, G. Ihorst, U. Kapp, BM cells giving rise to MSC in culture have a heterogeneous CD34 and CD45 phenotype, Cytotherapy 9(5) (2007) 439-50.
[64] M.F. Griffin, A. Ibrahim, A.M. Seifalian, P.E.M. Butler, D.M. Kalaskar, P. Ferretti, Chemical group-dependent plasma polymerisation preferentially directs adipose stem cell differentiation towards osteogenic or chondrogenic lineages, Acta Biomaterialia 50 (2017) 450-461.
[65] X. Liu, Q. Feng, A. Bachhuka, K. Vasilev, Surface chemical functionalities affect the behavior of human adipose-derived stem cells in vitro, Applied Surface Science 270 (2013) 473-479.
[66] H. Caplan, S.D. Olson, A. Kumar, M. George, K.S. Prabhakara, P. Wenzel, S. Bedi, N.E. Toledano-Furman, F. Triolo, J. Kamhieh-Milz, G. Moll, C.S. Cox, Jr., Mesenchymal Stromal Cell Therapeutic Delivery: Translational Challenges to Clinical Application, Front Immunol 10(1645) (2019) 1645.
[67] G. Brooke, M. Cook, C. Blair, R. Han, C. Heazlewood, B. Jones, M. Kambouris, K. Kollar, S. McTaggart, R. Pelekanos, A. Rice, T. Rossetti, K. Atkinson, Therapeutic applications of mesenchymal stromal cells, Seminars in Cell & Developmental Biology 18(6) (2007) 846-858.
[68] S. Jung, K.M. Panchalingam, R.D. Wuerth, L. Rosenberg, L.A. Behie, Large-scale production of human mesenchymal stem cells for clinical applications, Biotechnology and Applied Biochemistry 59(2) (2012) 106-120.
[69] I. Papantoniou, T. Lambrechts, J.-M. Aerts, Bioprocess engineering strategies for autologous human MSC-based therapies: one size does not fit all, Cell and Gene Therapy Insights 3(6) (2017) 469-482.
[70] A.M. Trimukhe, K.N. Pandiyaraj, A. Tripathi, J.S. Melo, R.R. Deshmukh, Plasma Surface Modification of Biomaterials for Biomedical Applications, in: A. Tripathi, J.S. Melo (Eds.), Advances in Biomaterials for Biomedical Applications, Springer Singapore, Singapore, 2017, pp. 95-166.
[71] M.C. Vasudev, K.D. Anderson, T.J. Bunning, V.V. Tsukruk, R.R. Naik, Exploration of Plasma-Enhanced Chemical Vapor Deposition as a Method for Thin-Film Fabrication with Biological Applications, ACS Applied Materials & Interfaces 5(10) (2013) 3983-3994.
[72] C.C. Barrias, M.C.L. Martins, G. Almeida-Porada, M.A. Barbosa, P.L. Granja, The correlation between the adsorption of adhesive proteins and cell behaviour on hydroxyl-methyl mixed self-assembled monolayers, Biomaterials 30(3) (2009) 307-316.